Cold Drawing-Induced Mesophase in Amorphous Poly(ethylene naphthalate) Revealed by X-ray Microdiffraction

M. C. García Gutiérrez,*,† J. Karger-Kocsis,‡ and C. Riekel†

European Synchrotron Radiation Facility, BP 220, F-38043 Grenoble Cedex, France, and Institut für Verbundwerkstoffe GmbH, Universität Kaiserslautern, Pf 3049, D-67653 Kaiserslautern, Germany

Received March 25, 2002; Revised Manuscript Received June 3, 2002

ABSTRACT: The structural changes occurring along the necked region developed when amorphous poly(ethylene naphthalate) (PEN) films are cold drawn were investigated by means of X-ray microdiffraction using synchrotron radiation. The wide-angle X-ray scattering (WAXS) results reveal the appearance of smectic order with a period of 1.25 nm corresponding to a chain repeat length associated with a sinusoidal conformation of the polymer chains (β-conformation), 5% shorter than that repeat length consisting in molecular chains showing the more extended α-conformation. The smectic order gradually decreases with increasing the distance from the tip of the necked region, showing a discontinuity, which corresponds to the transition zone between the necked region and the bulk, where molecular order suddenly drops. The small-angle X-ray scattering (SAXS) measurements give no indication that the mesophase is associated with a particular microstructure; however, the SAXS equatorial maximum presented at specific positions of the necked region may be related to the formation of small amount of crazelike structures produced by the intersections of shear bands, with shear banding and shear yielding being the mean deformation behavior as it is supported by scanning electron microscopy (SEM) micrographs. The necked zone induced by cold drawing partially disappears although not completely after annealing, and the residual chain orientation suggests that either the annealing conditions selected were not enough for a full recovery or that a material fraction has undergone plastic deformation.

Introduction

Poly(ethylene-2,6-naphthalate) (PEN) having rigid bulky naphthalene rings in its backbone is a relatively new member of the family of thermoplastic polyesters. PEN possesses higher stiffness, higher melting and glass transition (T_g) temperatures, and better barrier properties than poly(ethylene terephthalate) (PET). On the basis of this property profile, PEN is a promising candidate for various packaging applications, especially where hot filling and good barrier properties are required (e.g. containers, hollow bodies, bottles). The related products are usually produced by thermoforming and extrusion blow molding operations in which often uni- and biaxial orientations are involved. PEN is solidified during the processing in its amorphous phase. Some of the shaping steps may also occur below the T_g, which necessitates studying the stretching-induced alteration in the morphology to which this work was devoted. Note that while hot drawing-induced structural changes in PEN fibers and films has been extensively studied,[1,2] the cold-drawing process has been almost never studied. It was recently reported that the drawability of amorphous PEN strongly depends on the molecular weight of the resin and strain rate of the mechanical test adopted. It was shown that the necking behavior of a PEN of high molecular weight under high deformation rates agrees with that of a lower molecular weight resin under low deformation rates.[3,4] On the other hand, no reliable information is available on changes in the amorphous phase and on the onset of a possible strain-induced crystallization. That was the motivation of this study. Scanning X-ray microdiffraction with beam sizes of a few micrometers[5] allows the recording of high-quality simultaneous WAXS and SAXS patterns during mapping accurately the region of interest of the sample and allows us to follow the length scale of the deformation.

* Corresponding author. Tel: 33-(0)4 76 88 29 52. Fax: 33-(0)4 76 88 20 34. E-mail: mcgarcia@esrf.fr.

† European Synchrotron Radiation Facility. E-mail for J.K.-K.: karger@ivw.uni-kl.de.

‡ Universität Kaiserslautern. E-mail for C.R.: riekel@esrf.fr.

Experimental Section

Materials and Methods. Amorphous PEN films with a thickness of ca. 0.5 mm were supplied by the Eastman Chemical Co., Kingston, TN. An inherent viscosity of 0.899 dL/g was determined at 25 °C using a solution containing 0.5 g of polymer/100 mL of a 60/40 pentafluorophenol/trichlorobenzene mixture. A stressed deeply double-edge notched (DDEN-T) specimen was prepared in tensile fracture at room temperature using a crosshead speed of 1 mm min^{-1}.[6] A schematic picture of the fractured DDEN-T specimen is shown in Figure 1; a real specimen is shown elsewhere.[6] The temperature rise detected during loading of the DDEN-T specimens was less than 5 °C,[6] so that the glass transition temperature of PEN (ca. 118 °C) was not reached. The deformation of the glassy PEN polymer should therefore have occurred via cold drawing and not by true plastic deformation. A simple way to check the onset of cold drawing is by keeping the broken DDEN-T specimens for a few minutes just above T_g; the plastic zone should disappear, and the original shape of the DDEN-T specimen half should be mostly restored when the deformation mode was cold drawing.[7,8] This was the case, in fact, as has been reported in ref 1 and is schematically represented in Figure 1 (bottom). The necked region developed during loading is the subject of this X-ray diffraction study.

X-ray Diffraction. X-ray diffraction experiments were performed at the European Synchrotron Radiation Facility (ESRF) microfocus beamline (ID13) using a wavelength of 0.09755 nm (Si-111 monochromator) and a 5 μm diameter beam from a postcollimator.[5] Diffraction patterns were recorded with a CCD detector with 130 mm converter screen (MAR; 64.45 × 64.45 μm^2 pixels; 16-bit readout). Both WAXS and SAXS experiments were performed. The distance sample-to-detector was calibrated by an Ag−behenate sample as $D =$

10.1021/ma020468h CCC: $22.00
Published on Web 08/09/2002

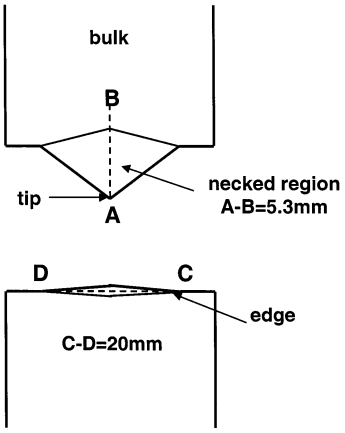

Figure 1. Schematic picture of a failed DDEN-T specimen of glassy PEN before (top) and after annealing (bottom) just above T_g. The recording positions of the WAXS and SAXS patterns (lines A−B and C−D) are shown.

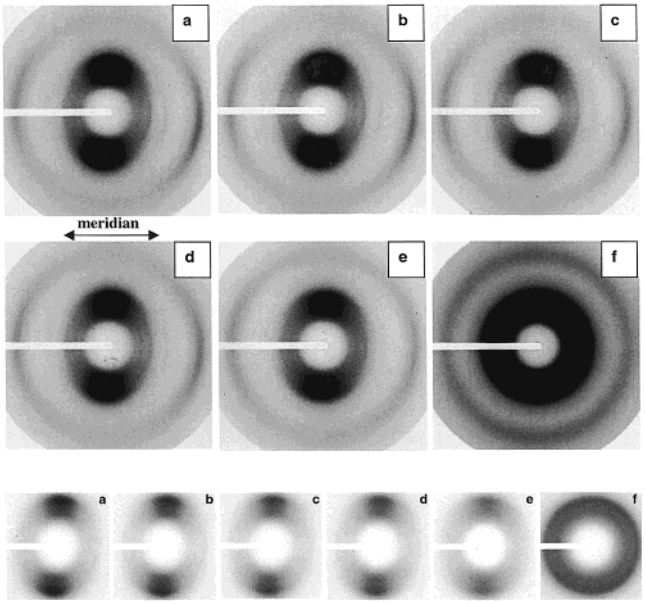

Figure 2. WAXS patterns recorded along the line AB (Figure 1, top), mapping the necked region from the tip to the bulk (top). The central part of WAXS patterns shows gradations in the equatorial reflections (bottom).

95.87 mm (WAXS) and D = 516.48 mm (SAXS). The lower limit in s ($s = 2(\sin\theta)/\lambda$) was $s_{min} = 0.015$ nm^{-1}.[9] Typical recording times were 60 s. Experiments were performed in air at T = 25 °C.

The sample was aligned on a goniometer head so that the line A−B (Figure 1) was nearly horizontal. A specific point of the sample was selected by a microscope and then transferred into the center of the X-ray beam at the exit of the collimator by a three-axis gantry, which was interfaced by computer-controlled motion software.[5] The sample was scanned through the beam with 500 or 20 μm steps. At every position a diffraction pattern was recorded in transmission. For background correction a pattern without sample was recorded. Data analysis was performed with the FIT2D software package.[10] Gaussian functions were fitted to the radial and azimuthal intensity profiles.

Results

Wide-Angle X-ray Scattering. Figure 2 shows a series of selected WAXS patterns obtained at distances of 1 mm along the line A−B (Figure 1, top), mapping the necked region from the tip to the bulk. The WAXS patterns from the necked region (Figure 2a−e) have a broad maximum centered on the equator while the pattern from the bulk shows a ring-shaped broad halo associated with an isotropic amorphous material (Figure 2f). The occurrence of a diffuse equatorial diffraction maximum in the necked region indicates that PEN molecules are preferentially aligned parallel to the draw direction with absence of crystalline order.

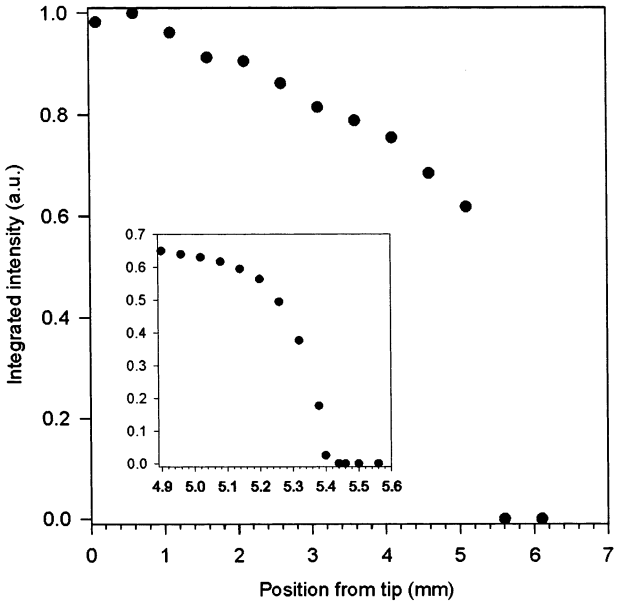

Figure 3. Variation of integrated intensities of the equatorial reflection as a function of position across the necked zone (line A−B in Figure 1). Inset: mapping more in detail the transition zone between the necked region and the bulk.

The equatorial peak allows determining the evolution of the oriented phase from the center of the edge of the necked region to the bulk by determining its integrated intensity as a function of position. For such a purpose the azimuthal profile of the equatorial reflection was fitted by a Gaussian function associated with the oriented phase and a polynomial background corresponding to the isotropic fraction (e.g. the azimuthal profile at the equator of the pattern from the bulk (Figure 2f) is only fitted by a polynomial background). The result (Figure 3) shows a continuous decrease of the volume fraction of the oriented phase with increasing the distance from the tip. A strong intensity jump occurs at a distance of 5 mm, corresponding to the transition zone between the necked region and the bulk. A higher resolution scan of the transition zone with 20 μm steps is shown in the inset of Figure 3.

In addition to the equatorial scattering a number of weak and relatively sharp reflections appear on the meridian (Figure 2a−d). These reflections do not correspond to that reported for either conventional semicrystalline[11−13] or amorphous PEN. A similar finding was referred by Jakeways et al.[1] as a mesophase that coexists with the conventionally ordered crystalline material and the disordered amorphous material to a greater or lesser degree in melt-spun PEN fibers drawn at 120 °C. More recently, Welsh et al.[2,14] reported a transient mesophase during hot drawing of PET and PEN and their associated random copolymers.

Figure 4 shows the radial profile of the meridional reflections of the WAXS pattern of Figure 2a. We assumed that meridional intensity profile consists of a series of narrow Gaussian functions and a short-range-

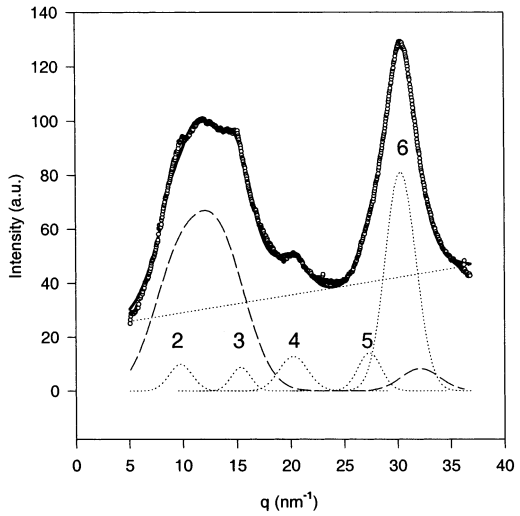

Figure 4. Radial profile of the meridional reflections of the WAXS pattern of Figure 2a, showing the mesophase structure.

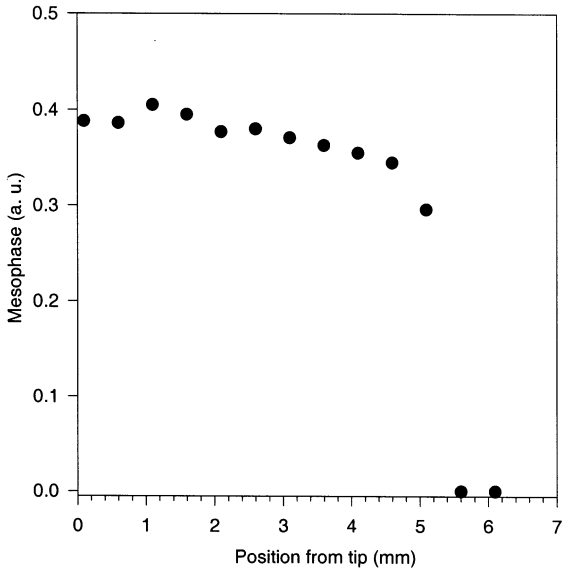

Figure 5. Integrated intensity of the meridional reflections identified with the mesophase, as a function of position along the line A−B in Figure 1.

order peak. For profile fitting we used an amorphous halo, obtained from a pattern that does not show a mesophase, and 5 Gaussian functions for the more narrow peaks. The analysis of the profile fit allows us to interpret the series of peaks as several reflection orders corresponding to a chain repeat length of 1.25 ± 0.02 nm. The order is noted in Figure 4 against each peak; the first order is not shown due to the experimental setup. The variation of the integrated intensity of the meridional reflections is shown in Figure 5. It is seen that the mesophase has the same behavior as the volume concentration of the oriented phase along the draw direction. Above about 5.5 mm the molecular orientation has disappeared.

The almost shape-restored necked region after the annealing treatment was scanned with 1 mm increments along line C−D (Figure 1, bottom) to verify the assumption of cold drawing. A sequence of WAXS patterns (Figure 6) shows that the broad maximum centered on the equator persists which suggests that either the annealing conditions selected were not enough for a full recovery or that a fraction of the material has

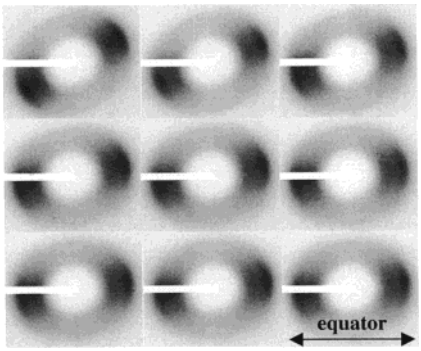

Figure 6. Central part of WAXS patterns recorded along the line C−D (Figure 1, bottom), mapping from the edge to the center of the partially shape restored necked region.

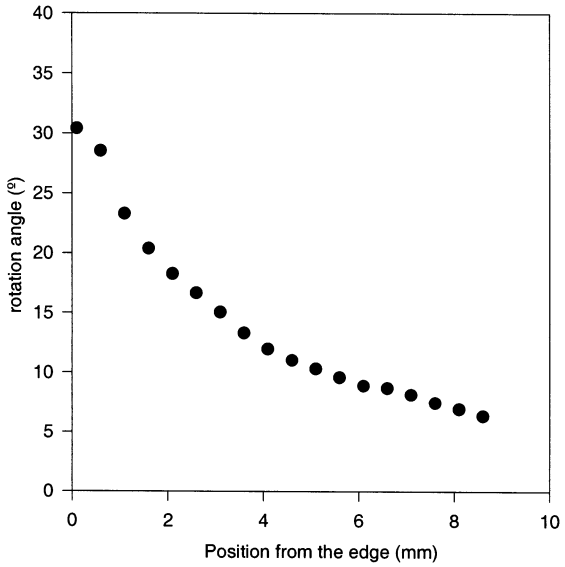

Figure 7. Variation of the angle of rotation of the maximum center on the equator from the horizontal line as a function of position along line C−D.

undergone plastic deformation. Plotting the angle of rotation of the equator from line C−D can also show the remaining macroscopic distortion. Figure 7 shows that this angle decreases with increasing distance from the edge (point C in Figure 1 (bottom)). Residual chain orientation in the shape-restored necked region was investigated by fitting a Gaussian function to the azimuthal profile of the equatorial reflection. Figure 8 illustrates the variation of relative azimuthal width at half of the maximum intensity with the distance from the edge (point C).

Small-Angle X-ray Scattering. Figure 9 shows a series of selected SAXS patterns obtained at distances of 0.5 mm along the line AB (Figure 1, top), mapping the necked region from the tip to the bulk. At some specific positions of the necked region (Figure 9a−j, top), SAXS patterns have a maximum centered on the equator while those of the bulk present a very weak isotropic scattered intensity (Figure 9k,l, top). The maximum centered on the equator, for some of the SAXS patterns, cannot be associated with the high chain orientation indicated by WAXS because such a maximum appears only at some specific positions of the necked region, while the mesophase and the volume concentration of the oriented phase along the draw direction, pointed out by WAXS, show a continuous decrease with increasing the distance from the tip of

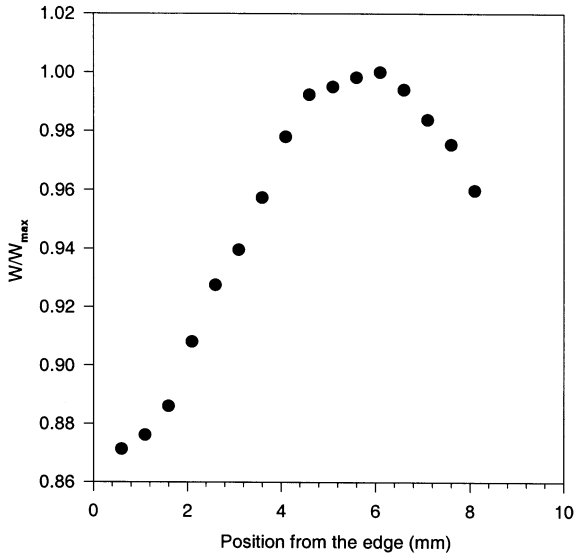

Figure 8. Relative azimuthal width at half of the maximum intensity W/W_{max} (scaled to maximum width of the reflection $W_{max} = 1$) as a function of the distance from the edge C.

the necked zone. Thus, the SAXS equatorial maximum should be related to the formation of crazelike structures, as it will be discussed below.

Discussion

Molecular Order by Cold Drawing. We have shown that cold drawing of glassy PEN at room temperature through necking induces preferential alignment of the chain axis along the draw direction. The chain repeat length of 1.25 nm derived from the meridional reflections is almost equal to the monomer unit length.[15] This suggests that neighboring molecular segments laterally tend to form layers orthogonal to the draw direction. The absence of crystalline order in the interchain packing means that the cold drawing-induced order in PEN can be classified as smectic. Jakeways et al.[1] reported the existence of a mesophase in PEN fibers prepared by spinning at a wind up speed of 500 m/min followed by drawing at 120 °C, where the odd numbered orders were considerably more intense than the even orders, and giving a value for the chain repeat length of 1.30 nm. These apparent discrepancies can be explained taking into account the different materials used and especially the different conditions used for the deformation process applied to the materials. Thus, the occurrence of so-called trans α- and β-conformations of the naphthalene rings in the crystalline and amorphous states of PEN is known. Monomer units containing the α-conformation are almost 5% longer than those having the more sinusoidal β-conformation (lengths 1.32 and 1.26 nm, respectively).[15] van den Heuvel et al.[15] reported a gradually $\beta \rightarrow \alpha$ transition in PEN yarns cold drawn at high draw ratios and a much more straightforward $\beta \rightarrow \alpha$ transition if the drawing is carried out at high temperature. This implies that the smectic order induced in PEN films by cold drawing is associated with a sinusoidal conformation of the polymer chains (β-conformation). In contrast, the mesophase reported by Jakeways et al. in melt-spun PEN fibers drawn at 120 °C, with a longer chain repeat length, would consist in molecular chains showing the more extended α-conformation. The role of chain conformation in the mesomorphic form of PET was also reported by Auriemma et al.[16]

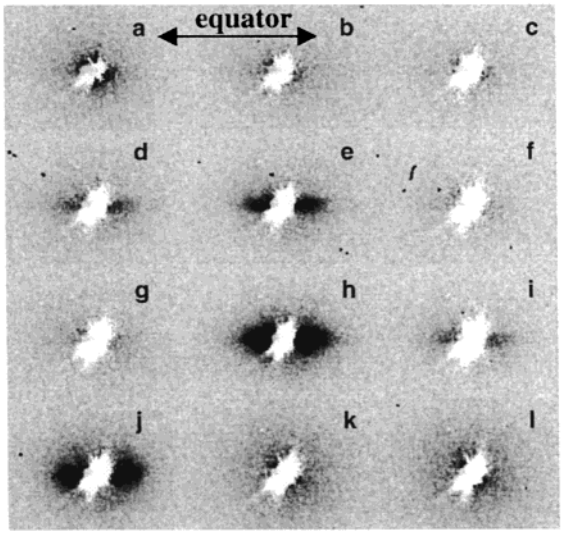

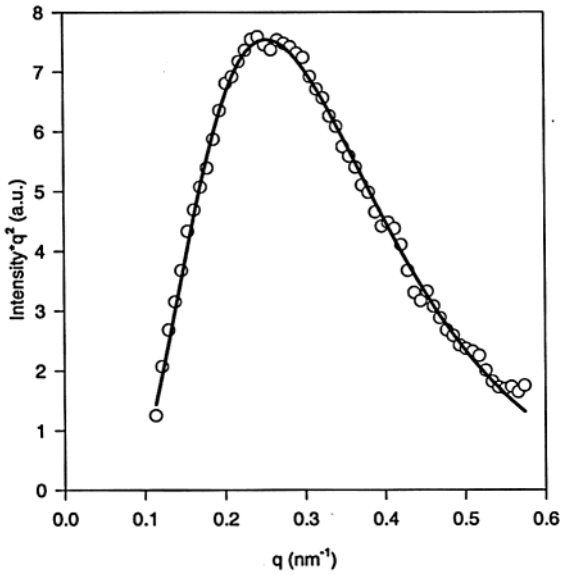

Figure 9. SAXS patterns recorded along the line A−B (Figure 1, top), mapping the necked region from the tip to the bulk (top), and a profile of the equatorial maximum of pattern h (bottom).

It is interesting to note that both the order along the draw direction, given by the variation of the broad maximum centered on the equator (Figure 3), and the lateral order orthogonal to the draw direction, characterized by the variation of meridional reflections (Figure 4), follow a slow and gradual decrease with increasing the distance from the tip of the necked region, showing a discontinuity at a distance of 5 mm, which corresponds to the transition zone between the necked region and the bulk, where molecular order suddenly drops.

Effects of Annealing. As it was pointed out previously, after the broken DDEN-T specimens were kept for a few minutes just above the glass transition temperature of PEN, the necked region apparently disappears and the original shape of the DDEN-T specimen half is macroscopically mostly restored. For mapping with the microbeam along the line CD (Figure 1, bottom) from the edge to the center of the shape restored necked region, it is seen that the angle of rotation of the equator from horizontal line decreases with increasing the distance from the edge (Figure 7). The physical origin of this rotation is due to an in-

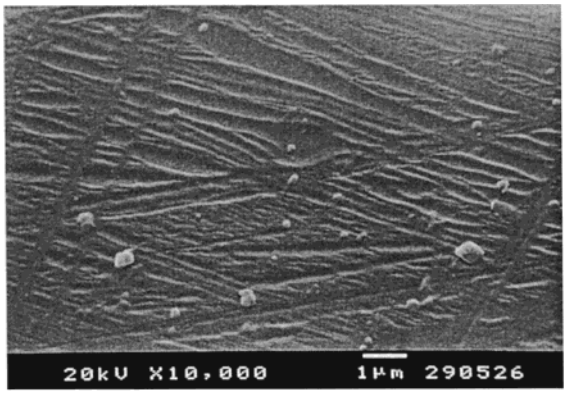

Figure 10. Scanning electron micrograph showing diffuse shear bands on the surface of the necked zone developed in cold drawn PEN.

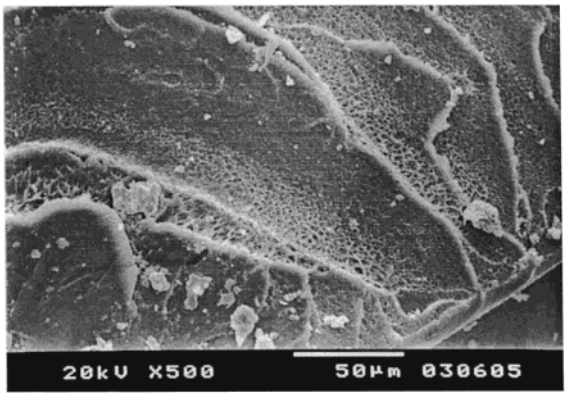

Figure 11. SEM micrograph of the fracture surface of cold drawn PEN along a big shear band.

homogeneous material flow in the necked zone during deformation owing to an instability in the crack growth prior to final fracture due to the deeply double-edge-notched (DDEN) specimen geometry used.[17] What is most interesting is the fact that the variation of relative azimuthal width at half of the maximum intensity along the line CD seems to be symmetric showing a maximum at the middle point (Figure 8), a fact that suggests a higher orientation of the polymer chains at the edges (points C and D) than at the center of the necked region. This statement is supported by the microhardness measurements carried out in a sample prepared in the same way as in the present investigation,[18] where the hardness reaches its maximum values at points C and D and decreases nearly continuously from the right and left edges of the necked zone toward the center.

Yielding Mechanisms in the Necked Zone. From all the observations on various polymeric solids, it has become clear that there are two mechanisms of yielding.[19] The first one is known as "shear yielding", which is the mean deformation behavior of cold drawn PEN as it is supported by the SEM micrograph of the necked zone (Figure 10). The second mechanism of yielding is called "crazing"; crazes are zones plastically deformed, 50−100 μm in length and 0.1−2 μm wide, and highly oriented polymeric material mainly consisting of fibrils, 20−30 nm apart and 5−30 nm in diameter, along the direction of applied stress.[20] Transmission X-ray scattering from the orthogonal craze walls and fibrils results in highly anisotropic patterns, having the form of two elongated streaks approximately perpendicular to each other. The maximum developed at the equator indicating the regular arrangement of fibrils and the streak

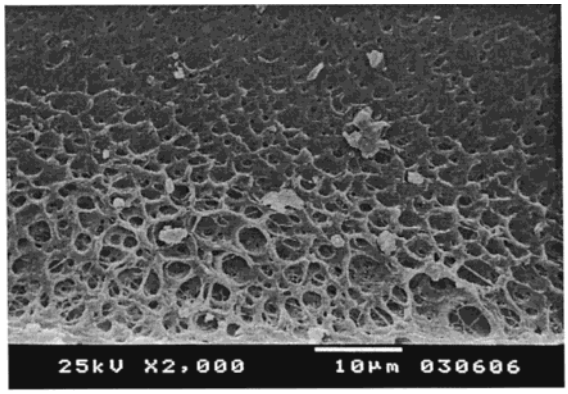

Figure 12. Higher magnification of the fibrillated crazelike structure produced by the intersections of shear bands shown in Figure 11.

at the meridian is the scattering from craze walls.[21,22] The SAXS patterns observed in the present investigation, depending on their taken position of the necked region (Figure 9a−j, top), have a maximum centered on the equator with an average long period of 25 nm (Figure 9, bottom) that could correspond either to the fibril distance or to the fibril diameter of a fibrillated crazelike structure produced by the intersections of shear bands as it can be seen in the SEM micrographs of the fracture surface of PEN along a big shear band (Figures 11and 12). The meridional streak is not seen because the SAXS resolution of the instrument used is not high enough.

Conclusions

On the basis of the X-ray diffraction study of cold-drawn PEN, we may draw the following conclusions:

(i) Although already understood for hot-drawn PEN materials, we report for the first time cold drawing-induced mesophase in glassy PEN.

(ii) The mesophase is apparent from WAXS patterns, its signature being comparatively weak yet relatively sharp meridional peaks, corresponding to a chain repeat length of 1.25 ± 0.02 nm, associated with a sinusoidal conformation of the polymer chains (β-conformation), 5% shorter than that repeat length consisting in molecular chains showing the more extended α-conformation.

(iii) Cold drawing of glassy PEN at room temperature through necking induces a mesophase order consistent with that of smectic, since the neighboring molecular segments laterally tend to form layers orthogonal to the draw direction with absence of crystalline order in the interchain packing.

(iv) The necked region induced by cold drawing partially disappears although not completely after keeping the broken DDEN-T specimens for a few minutes just above the glass transition temperature of PEN. The residual chain orientation suggests that a fraction of the material has undergone plastic deformation, the stretched entanglement network has been disrupted in certain points, and a small amount of fibrillated crazelike structures are produced by the intersections of shear bands in the necked region.

Acknowledgment. M.C.G.G. acknowledges the generous support of this investigation by a European Community Marie Curie Fellowship.

References and Notes

(1) Jakeways, R.; Klein, J. L.; Ward, I. M. *Polymer* **1996**, *37*, 3761−3762.
(2) Welsh, G. E.; Blundell, D. J.; Windle, A. H. *Macromolecules* **1998**, *31*, 7562−7565.
(3) Karger-Kocsis, J. Fracture and fatigue behaviour of amorphous (co)polyesters as a function of molecular and network variables. In *Handbook of Thermoplastic Polyesters*; Fakirov, S., Ed.; Wiley-VCH: Weinheim, Germany, 2002 (in press).
(4) Karger-Kocsis, J.; Czigány, T. *Polym. Eng. Sci.* **2000**, *40*, 1809−1815.
(5) Riekel, C. *Rep. Prog. Phys.* **2000**, *63*, 233−262.
(6) Karger-Kocsis, J.; Moskala, E. J. *Polymer* **2000**, *41*, 6301−6310.
(7) Karger-Kocsis, J.; Czigány, T.; Moskala, E. J. *Polymer* **1998**, *39*, 3939−3944.
(8) Karger-Kocsis, J.; Moskala, E. J. *Polym. Bull.* **1997**, *39*, 503−510.
(9) Riekel, C.; Burghammer, M.; Müller, M. *J. Appl. Crystallogr.* **2000**, *33*, 421−423.
(10) Hammersley, A. FIT2D Website. http://www.esrf.fr/computing/expg/subgroups/data•analysis/FIT2D/index/html.
(11) Mencik, Z. *Chem. Promsyl.* **1967**, *17*, 78−83.
(12) Buchner, S.; Wiswe, D.; Zachmann, H. G. *Polymer* **1989**, *30*, 480−488.
(13) Nakamae, K.; Nishino, T.; Gotoh, Y. *Polymer* **1995**, *36*, 1401−1405.
(14) Welsh, G. E.; Blundell, D. J.; Windle, A. H. *J. Mater. Sci.* **2000**, *35*, 5225−5240.
(15) van den Heuvel, C. J. M.; Klop, E. A. *Polymer* **2000**, *41*, 4249−4266.
(16) Auriemma, F.; Corradini, P.; De Rosa, C.; Guerra, G.; Petraccone, V.; Bianchi, R.; Di Dino, G. *Macromolecules* **1992**, *25*, 2490−2497.
(17) Karger-Kocsis, J. *Polym. Eng. Sci.* **1996**, *36*, 203−210.
(18) Krumova, M.; Karger-Kocsis, J. *Int. J. Polym. Mater.* **2001**, *50*, 321−333.
(19) Strobl, G. In *The Physics of Polymers: Concepts for Understanding their Structures and Behaviour*; Strobl, G., Ed.; Springer-Verlag: Berlin, Heidelberg, 1996; p 349.
(20) Michler, G. H. *Colloid Polym. Sci.* **1989**, *267*, 377−388.
(21) Lode, U.; Pomper, T.; Karl, A.; von Krosigk, G.; Cunis, S.; Wilke, W.; Gehrke, R. *Macromol. Rapid. Commun.* **1998**, *19*, 35−39.
(22) Salomons, G. J.; Singh, M. A.; Bardouille, T.; Foran, W. A.; Capel, M. S. J. *Appl. Crystallogr.* **1999**, *32*, 71−81.

MA020468H